Polyacene Spacers in Intramolecular Magnetic Coupling

2 AUTHORS:

Md. Ehesan Ali
Institute of Nano Science and Technology
26 PUBLICATIONS   515 CITATIONS

SEE PROFILE

Sambhu N Datta
Indian Institute of Technology Bombay
128 PUBLICATIONS   947 CITATIONS

SEE PROFILE

Polyacene Spacers in Intramolecular Magnetic Coupling

Md. Ehesan Ali and Sambhu N. Datta*

Department of Chemistry, Indian Institute of Technology—Bombay, Powai, Mumbai-400076, India

Received: May 31, 2006; In Final Form: September 26, 2006

We predict the intramolecular magnetic exchange coupling constant (J) for eleven nitronyl nitroxide diradicals (NN) with different linear and angular polyacene couplers from broken-symmetry density functional treatment. For the linear acene couplers, J initially decreases with increase in the number of fused rings. But from anthracene coupler onward, the J value increases with the number of benzenoid rings due to an increasing diradical character of the coupler moiety. The J value for the diradical with a fused bent coupler is always found to be smaller than that for a diradical with a linear coupler of the same size. The nuclear independent chemical shift (NICS) is calculated, and it is observed that the average of the NICS values per benzenoid ring in the diradical is less than that in the normal polyacene molecule. An empirical formula for the magnetic exchange coupling constant of a NN diradical with an aromatic spacer is obtained by combining the Wiberg bond order (BO), the angle of twist (ϕ) of the monoradical (NN) plane from the plane of the coupler, and the NICS values. A comparison of the formula with the computed values reveals that, from tetracene onward, the diradical nature of the linear acene couplers becomes prominent thereby leading to an increase in the ferromagnetic coupling constant. Isotropic hyperfine coupling constants are calculated by using a polarized continuum model for the diradicals in different solvents and in vacuum.

1. Introduction

Design and synthesis of ferromagnetic materials based on organic molecules have started attracting experimental as well as theoretical attention. Magnetic properties of a molecule-based material are controlled by intramolecular and intermolecular magnetic exchange coupling constants. The latter depend upon the structure of the molecule and also on the nature of the molecular crystal.[1] The knowledge of the intramolecular exchange coupling constant is often crucial before making an attempt to synthesize a successful ferromagnetic material based on organic diradicals. This creates an interest in the aromatic fused-ring couplers, as the latter are easily available and can be varied in length and topology.

Nitronyl nitroxide (NN) radicals have become the natural choice in molecular magnetism since they are stable at ordinary conditions of temperature and pressure and also have cooperative magnetic properties.[2] These radicals are well characterized from structural and spectroscopic viewpoints. The strong localization of the unpaired electron of NO makes the NN radicals ideal ferromagnetic precursors.[3] The first example of a pure organic ferromagnetic material is the β-crystal phase of *p*-nitrophenyl nitronyl nitroxide.[4,5] A large number of NN radicals have been investigated. Recently, Turek et al.[6] have theoretically investigated a series of *m*-phenylene couplers and shown that the influence of spin polarization and molecular conformation controls the exchange coupling constant. Barone et al.[7] have theoretically investigated bis(imino) nitroxide and concluded that most of the spin density along the O−N−C−N moiety of each monomeric unit can be attributed to the unpaired electron in the singly occupied molecular orbital (SOMO). This implies that a coupler that is extensively conjugated can give rise to a strong magnetic interaction between the monomeric radical centers. Ziessel et al.[8] synthesized a nitronyl nitroxide diradical

with the ethylenic coupler, which shows a very high antiferromagnetic coupling constant. We have justified it theoretically.[9] In a previous work, we have noticed that the π-conjugated linear spacers are, as couplers, stronger than the aromatic ones.[10] We have also noticed that the aromaticity of the coupler plays a major role in controlling the strength of magnetic interaction. The *m*-phenylene species is known to be one of the best ferromagnetic couplers. In the present work, we investigate the magnetic properties of eleven ferromagnetically coupled NN diradicals with linear and angular polyacene couplers (Figure 1). The polyacenes are aromatic hydrocarbons with benzenoid rings. They have been extensively investigated for their electronic properties, molecular structure, and aromaticity. Pentacene has attracted a special attention as an active organic semiconductor molecule.[11] The larger polyacenes are predicted to be conductors with nearly zero band gap.[12] The objective of this work is to investigate the intramolecular ferromagnetic interaction mediated by polyacene spacers.

The magnetic interaction in organic radicals generally arises from spin polarization and spin delocalization. Lahti et al.[13] have investigated a large number of π-conjugated couplers. They have noticed that most of the spin density is localized on the two singly occupied σ orbitals (SOMOs) centered on the radical atoms. The large spin population polarizes the π-electrons near the radical center. The presence of nonbonding molecular orbitals (NBMOs) in organic diradicals makes it difficult to properly evaluate the energy difference between the lowest spin states. The expected ground state spin may be predicted either by a molecular orbital (MO) calculation or by a valence bond (VB) treatment. A number of derivations were made to model the intramolecular exchange in connectivity-conjugated systems by Ovchinikov,[14] Klein,[15] Borden and Davidson,[16] and Sinanŏglu.[17] A large number of computational studies have also been performed.[18] It is generally observed that the spin polarization argument is more useful to understand the spin density distribution in an open-shell system.

* Author to whom correspondence should be addressed. E-mail: sndatta@chem.iitb.ac.in.
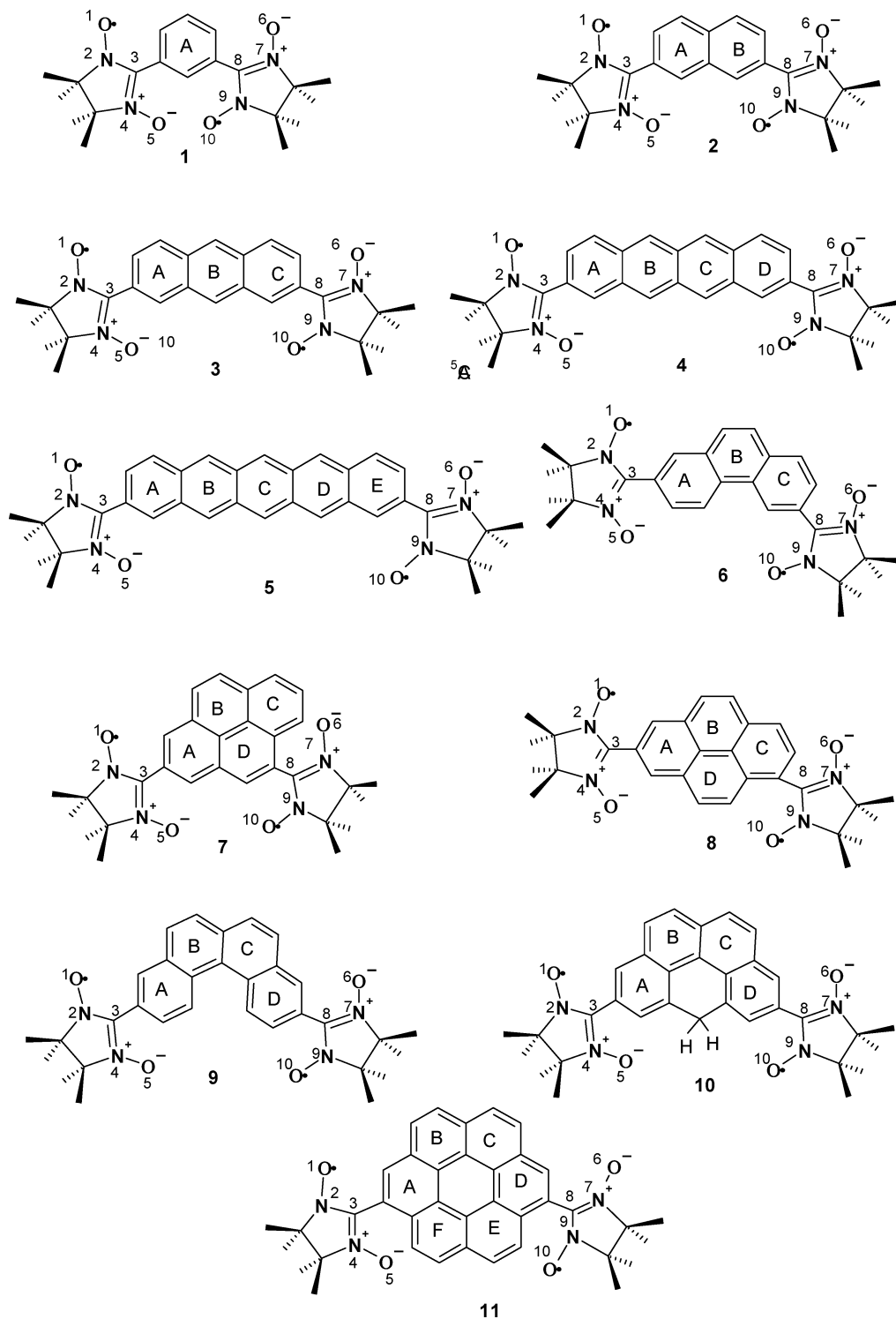
Figure 1. Diradicals under investigation.

In this work we rely on the spin-polarized DFT methodology to calculate the magnetic exchange coupling constants. The broken-symmetry (BS) approach that was proposed by Noodleman et al.[19] is adopted here.

2. Theoretical Background

The magnetic exchange interaction between two magnetic sites 1 and 2 is normally expressed by the Heisenberg effective spin Hamiltonian

$$\hat{H} = -2J\hat{S}_1 \cdot \hat{S}_2 \qquad (1)$$

where $\hat{S}_1$ and $\hat{S}_2$ are the respective spin angular momentum operators. A positive sign of J indicates a ferromagnetic interaction, whereas the negative sign indicates an antiferromagnetic interaction. The eigenfunctions of the Heisenberg Hamiltonian are eigenfunctions of $\hat{S}^2$ and $\hat{S}_z$ where S is the total spin angular momentum and J is directly related to the energy difference between the spin eigenstates. For a diradical,

$$E(S=1) - E(S=0) = -2J \qquad (2)$$

The magnetic exchange coupling constant can be evaluated by determining the proper singlet and triplet energy values from a

multiconfigurational approach. The single determinantal wave function fails to give a proper accounting of this exchange.

An alternative approach has been proposed by Noodleman so as to reliably estimate the magnetic exchange coupling constant with less computational effort.[19] The spin-polarized, unrestricted formalism and a broken-symmetry (BS) solution are needed for the lowest spin state in this method. The BS state is not an eigenstate of $\hat{H}$. It is an equal mixture of a singlet and a triplet state. The coupling constant can be written as

$$J^{(1)} = \frac{(E_{BS} - E_{T'})}{1 + S_{ab}^2} \quad (3)$$

where S_{ab} is the overlap integral between the two magnetic orbitals a and b. The quantity E_{BS} is the energy of the broken-symmetry solution, and $E_{T'}$ is the energy of the triplet state in the unrestricted formalism using the BS orbitals. In a single-determinant approach, $E_{T'}$ can be approximated by the energy of the triplet state that is achieved by a direct computation ($E_{T'} \approx E_T$), because of the much less spin contamination in the high-spin state. In contrast, the BS state is often found as spin-contaminated. Therefore, spin-projected methods have been applied to eliminate the effect of the spin contamination from the energy of the BS state. Equation 3 is valid when there is only one pair of magnetic orbitals. The following three spin-projected equations (eqs 4−6) are additional results obtained from the same basic methodology and valid for different general cases:

$$J^{(2)} = \frac{(^{DFT}E_{BS} - {}^{DFT}E_T)}{S_{max}^2} \quad (4)$$

$$J^{(3)} = \frac{(^{DFT}E_{BS} - {}^{DFT}E_T)}{S_{max}(S_{max} + 1)} \quad (5)$$

$$J^{(4)} = \frac{(^{DFT}E_{BS} - {}^{DFT}E_T)}{\langle S^2 \rangle_T - \langle S^2 \rangle_{BS}} \quad (6)$$

These three relations differ in their applicability that depends on the degree of overlap between the two magnetic orbitals. Equation 4 has been derived by Ginsberg,[20] Noodleman,[19] and Davidson[21] (GND) and is applied when the overlap of the magnetic orbitals is sufficiently small. Equation 5 has been proposed by GND, Bencini et al.,[22] and Ruiz et al.[23] Illas et al.[24] have justified the application of eq 5 when the overlap is adequately large. Finally, eq 6 has been developed by Yamaguchi et al.[25] This can be reduced to eq 4 and eq 5 in the weak and strong overlap regions respectively.

3. Computational Methodology

Molecular geometries are optimized at the ROHF level using 6-311G(d,p) basis sets. The magnetic exchange coupling constants are calculated using the spin-polarized unrestricted DFT methodology. The basis set used for this purpose is 6-311+G(d,p). The BS states are obtained by calculating the proper ROHF wave functions and using these as initial guesses in the UB3LYP calculations. All the calculations are performed by using the Gaussian 03 suite of programs.[26]

To study the effect of aromaticity of the coupler on the magnetic exchange interaction, the nucleus-independent chemical shift (NICS) values are calculated by B3LYP/GIAO methodology for all the aromatic rings in each diradical. The NICS values are calculated at the center of the rings

TABLE 1: Results from Single-Point Broken-Symmetry Calculations at UB3LYP/6-311+G(d,p) Levels and the Calculated J Values[a]

| diradical | energy (au) ($\langle S^2 \rangle$) | | $J^{(2)}$ (cm^{-1}) | $J^{(4)}$ (cm^{-1}) |
	BS	T		
1[b]	−1299.0066208	−1299.006716	20.89	20.78
	1.070268	*2.075584*		
2	−1452.68288294	−1452.68295337	15.46	15.39
	1.0706	*2.0754*		
3	−1606.35279897	−1606.35286055	13.52	13.44
	1.0720	*2.0775*		
4	−1760.02026569	−1760.02032912	13.92	13.81
	1.0742	*2.0821*		
5	−1913.68945590	−1913.68953368	17.07	16.73
	1.0767	*2.0910*		
6	−1606.32389842	−1606.32393844	8.78	8.76
	1.0946	*2.0974*		
7	−1682.60289023	−1682.60291783	6.06	6.05
	1.0706	*2.0726*		
8	−1682.60180740	−1682.60183056	5.08	5.07
	1.0683	*2.0701*		
9	−1760.03222796	−1760.03224969	4.77	4.76
	1.0825	*2.0842*		
10	−1798.16513473	−1798.16515225	3.85	3.84
	1.0707	*2.0722*		
11	−1988.76716320	−1988.76716712	0.86	0.86
	1.0660	*2.0663*		

[a] The triplet geometry is optimized. Legends: J(2) for GND eq 4 with $S_{max} = 1$, and J(4) from Yamaguchi eq 6. [b] These values are reported in ref 10, and the observed J value is 20 cm^{-1} (ref 30).

[NICS(0)]. But the σ framework of C−C and C−H affects the π-electrons, and hence NICS is also calculated at 1 Å above the ring [NICS(1)] where the π-electron density is known to be maximum.

The isotropic hyperfine coupling constant (hfcc), which is essential in experiment to characterize the radical systems and to predict the intramolecular exchange interaction, is also calculated at the B3LYP/EPR-II/C-PCM level. The hfcc values are first determined for the diradical in vacuum. EPR parameters are strongly solvent dependent. To account for the solvent effect, hfcc's are also calculated using the conductor-like polarizable continuum model (CPCM). Three solvents have been considered. These are the nonpolar solvent benzene ($\epsilon = 2.25$), the moderately polar and aprotic solvent acetonitrile ($\epsilon = 36.64$), and the polar and protic solvent water ($\epsilon = 78.39$).

4. Results and Discussion

Table 1 shows the calculation of J from eqs 4 and 6. The decreasing order of the J from **1** to **3** is in agreement with our general observation that magnetic exchange interaction in NN diradical with linear conjugated couplers decreases with the increase in the length of the coupler.[10] The reason for the deviation of **3**−**5** is that the larger oligoacenes possess open-shell singlet ground states,[27a] that is, these acenes are diradicals with disjoint nature.

The J value decreases remarkably for the bent couplers. The coupler in **6** has 3 fused rings. Those in **7**−**9** have 4 fused rings. The coupler in **10** has 4 fused aromatic rings and one fused nonaromatic ring, while that in **11** has 7 fused aromatic rings. One consequence of being bent is that the coupler fragments lose the disjoint diradical character. Also, they become stronger aromatics as discussed later. Diradicals **3** and **6** are similar, but J is much smaller for the phenanthrene coupler (**6**) than the anthracene one (**3**). The J value further decreases for the 1,8 and 1,7 substituted pyrene couplers (**7** and **8**). The couplers of

Polyacene Spacers in Intramolecular Magnetic Coupling

J. Phys. Chem. A, Vol. 110, No. 49, 2006 **13235**

TABLE 2: The Calculated Wiberg Bond Order at the B3LYP/6-311+G(d,p) Level for the NN− Coupler Bond and the Average Dihedral Angle between the NN and Coupler Planes

	bond order[a]			dihedral angle[b]		
diradical	r_1	r_2	average	ϕ_1	ϕ_2	average
1	1.05	1.05	1.05	34.74	32.33	33.54
2	1.07	1.07	1.07	25.76	25.78	25.77
3	1.08	1.07	1.08	26.45	22.87	24.66
4	1.07	1.08	1.08	26.87	22.71	24.79
5	1.07	1.08	1.08	27.06	22.61	24.84
6	1.07	1.05	1.06	5.72	43.65	24.68
7	1.07	1.02	1.05	23.01	54.22	38.61
8	1.07	1.03	1.09	22.90	53.87	38.38
9	1.07	1.07	1.07	24.22	23.16	23.69
10	1.07	1.07	1.07	23.96	25.22	24.59
11	1.02	1.02	1.02	55.32	55.31	55.31

[a] r_1 and r_2 are bond lengths between the benzenoid ring and the two NN radicals. [b] ϕ_1 and ϕ_2 are the angles of twist of the two NN moieties from the plane of the coupler.

diradicals **2** and **7** are similar, but the value of *J* for **2** is more than twice that for **7**. Again, **6** and **8** are similar in length except for an additional ring in **8**, but *J* is larger in **6** than in **8**. The same trend, that is, the decrease of the *J* value with the increase of conjugation in the bent aromatic coupler, is observed in the case of **9**−**11**. Nevertheless, conjugation within the coupler is not the only factor that determines the strength of the intramolecular exchange interaction.

Bond Order and Dihedral Angles. Wiberg bond index (order)[28] is calculated by natural bond orbital (NBO) analysis (implemented in Gaussian 03) at the B3LYP/6-311+G(d,p) level. The calculated bond orders are given in Table 2 along with the angle of rotation of the NN plane from the coupler plane (ϕ).

The average bond order (BO) for the linear acene couplers (**1**−**5**) increases with the increase of the number of phenyl rings in the coupler. A larger bond order generally favors greater conjugation with the radical centers, and hence a larger magnetic exchange coupling constant. The rotation of the NN plane from the plane of the coupler (ϕ) has an opposite effect, that is, if ϕ increases, *J* decreases because of the lesser conjugation. In **1**−**3**, *J* decreases although BO increases and ϕ decreases, whereas for **3**−**5**, *J* increases with the size of the coupler along with the increase in ϕ.

The planes of the two NN moieties are asymmetrically twisted for the angular diradicals **6**−**8**. One of the NN planes undergoes a large twist, and this fact is also reflected in BO. The BO and ϕ are consistent with the trend in calculated *J* values for the diradicals **6**−**8**, and a similar trend is observed for **9**−**11**. For the highly planar and conjugated coupler coronene (**11**), the much smaller *J* value (0.86 cm^{-1}) is due to the extremely large angle of twist ($\phi = 55.31°$), basically a stereoelectronic effect.

Nuclear Independent Chemical Shift (NICS). NICS(0) and NICS(1) are calculated at GIAO-B3LYP/6-311+G(d,p) level for different six membered rings in each coupler. NICS is an accepted measure of aromaticity. The benzenoid rings are denoted as A, B, C, etc. in Figure 1, and the corresponding values of NICS(0) and NICS(1) are given in Table 3.

The linear polyacene molecules have already been investigated by Schleyer et al.[29] using the same methodology and basis sets. These authors observed that the terminal rings have less benzenoid character as the size of the linear acene increases. For the angular acenes, however, the central rings have a reduced benzenoid character except in the thoroughly aromatic molecule

TABLE 3: The Calculated NICS Values at the Center of the Aromatic Rings for Diradicals 1−11

diradical	NICS	A	B	C	D
1	NICS(0)	−7.51			
	NICS(1)	−9.24			
2	NICS(0)	−7.60	−7.57		
	NICS(1)	−9.62	−9.68		
3	NICS(0)	−6.47	−10.3	−6.28	
	NICS(1)	−8.61	−12.22	−8.41	
4	NICS(0)	−5.15	−10.5	−10.38	−5.04
	NICS(1)	−7.51	−12.4	−12.29	−7.35
5[a]	NICS(0)	−3.87	−9.60	−11.40	−9.61
	NICS(1)	−6.62	−11.62	−13.64	−11.51
6	NICS(0)	−7.95	−4.66	−8.06	
	NICS(1)	−9.96	−7.72	−10.16	
7	NICS(0)	−10.41	−2.86	−10.85	−2.72
	NICS(1)	−12.19	−6.29	−12.58	−5.95
8	NICS(0)	−10.68	−2.82	−10.32	−2.93
	NICS(1)	−12.42	−6.38	−12.13	−6.33
9	NICS(0)	−8.04	−5.63	−5.61	−8.20
	NICS(1)	−8.85	−8.06	−8.81	−11.12
10	NICS(0)	−7.36	−5.21	−5.17	−7.49
	NICS(1)	−9.37	−8.06	−8.07	−9.48
11[b]	NICS(0)	− 8.65	−8.37	−8.50	−8.95
	NICS(1)	−10.87	−10.85	−10.92	−10.67

[a] NICS(0) and NICS(1) for ring E in species **5** are −3.87 and −6.34 respectively. [b] NICS(0) and NICS(1) for ring E in species **11** are −8.38 and −10.83 respectively and for ring F are −8.54 and −10.93.

TABLE 4: The Calculated NICS(1) Values for the Diradicals and the Corresponding Acene Molecules, ΔNICS(1), and the *J* Value Calculated from Eq 6 and Estimated from Eq 7

	average NICS(1)			$J^{(4)}$	*J*
diradical	couplers[a]	acenes[b]	ΔNICS(1)	eq 6	eq 7
1	−9.24	−10.60[c]	1.36	20.78	20.00
2	−9.56	−10.80[c]	1.15	15.39	13.10
3	−9.75	−11.00[c]	1.25	13.44	10.72
4	−9.89	−11.10[c]	1.21	13.81	8.22
5	−9.94	−11.20[c]	1.25	16.73	7.01
6	−9.28	−9.94[c]	0.66	8.76	5.42
7	−9.25	−10.62[d]	1.37	6.05	6.19
8	−9.32	−10.62[d]	1.30	5.07	5.95
9	−9.21	−9.59[d]	0.38	4.76	3.02
10	−8.75	−9.27[d]	0.52	3.84	4.23
11	−10.83	−12.17[d]	1.34	0.86	2.22

[a] In NN diradical. [b] Acene molecule without any NN radical as substituent. [c] Schleyer et al., ref 29. [d] Calculated at the GIAO-B3LYP/6-311+G(d,p) level, our work.

11. These trends are exactly preserved for the acene couplers in the diradicals under investigation (Table 3).

Table 4 shows that the average NICS(1) for a coupler is always less than that for the normal acene molecule. The difference between NICS(1) of a NN diradical and that of the corresponding acene molecule is written as ΔNICS. The loss of aromaticity in the coupler moiety is due to the participation of the conjugated π-electrons in the magnetic exchange phenomenon. We notice that *J* is proportional to the fractional change of NICS(1) from the parent acene, that is, ΔNICS: |NICS(1)| for acene. It is also generally proportional to the Wiberg bond order BO, cos ϕ_1, and cos ϕ_2. As we discussed in ref 10 for linear aliphatic couplers, the absolute magnitude of atomic spin density approximately varies as $1/(N + 1)$ where N is the number of conjugated atoms in the coupler, and *J* is approximately proportional to $1/(N + 1)$. Similarly, here, *J* will be further proportional to a factor of $1/(n + 1)$ where n is the number of benzenoid rings in the ployacene coupler. These

13236 *J. Phys. Chem. A, Vol. 110, No. 49, 2006*

Ali and Datta

TABLE 5: The SOMO−SOMO Energy Splitting at the UB3LYP/6-311+G(d,p) Level for the Triplet State

diradical	E(SOMO1) (au)	E(SOMO2) (au)	ΔE(SOMO) (au)
1	−0.19697	−0.19183	0.0051
2	−0.19836	−0.19831	0.0001
3	−0.19958	−0.19806	0.0015
4	−0.19920	−0.19421	0.0050
5	−0.19895	−0.18585	0.0131
6	−0.22288	−0.16391	0.0590
7	−0.19963	−0.18928	0.0104
8	−0.19970	−0.19223	0.0075
9	−0.19819	−0.18973	0.0085
10	−0.19837	−0.19778	0.0006
11	−0.19359	−0.19358	0.0000

TABLE 6: Calculated Average Isotropic Hyperfine Coupling Constant (hfcc) for Nitrogen Atoms of the Diradical in Different Environments

diradicals	gas phase	benzene	acetonitrile	water
1[a]	2.78	2.96	2.95	2.97
2	2.90	3.15	3.23	3.25
3	3.26	3.25	3.37	3.35
4	3.26	3.23	3.38	3.40
5	3.07	3.29	3.37	3.40
6	2.76	3.15	3.23	3.38
7	2.82	2.90	2.95	3.04
8	2.96	3.02	3.12	3.14
9	2.78	2.80	2.94	2.95
10	3.09	3.19	3.33	3.29
11	2.79	2.86	2.92	2.94

[a] Experimental data for **1** in 2-methyltetrahydrofuran give $a_N = 3.5$ G (ref 33d).

proportionalities can be coupled together to write the qualitative expression

$$J = A \times \frac{(\Delta\text{NICS})(\text{BO})\cos\phi_1\cos\phi_2}{(n+1)(\text{NICS})} \quad (7)$$

where NICS in the denominator is the absolute magnitude of NICS(1) for the parent acene. The proportionality constant A is found by considering the experimental value $J = 20$ cm^{-1} for the *m*-phenylene coupler (with $n = 1$).[30] We get $A = 426.5$ cm^{-1}. The J values calculated from eq 7 are given in Table 4. It is seen that eq 7 produces a rough estimate of J, but for the linear polyacenes, the estimate grows progressively worse from **3** to **5**.

For the linear acenes, the average NICS(1) per benzenoid ring increases with the size of the coupler (Table 4). It is also evident that the diradical character increases with the coupler size.[27a] Introducing the effective value $(1 - \chi_d)$NICS in place of NICS in the denominator of eq 7 for the diradicals with linear couplers, and using the scaling of the calculated J values by the multiplicative factor 0.9625 (=20.0/20.78), we find the deviation parameter χ_d as 0.0, 0.12, 0.17, 0.38, and 0.56 respectively for n equal to 1−5. The deviation parameter reflects the trend of the increasing diradical character.

The deviation cannot be straightforwardly applied to the bent couplers where the central rings are less aromatic. Also, the variation of NICS(1) is not smooth like that in linear couplers because of the zwitterionic contributions in bent acenes.[27b] The J values estimated by eq 7 in this case are generally in better agreement with the calculated values.

SOMO−SOMO Energy Splitting. The energies of the SOMOs are calculated at the UB3LYP/6-311+G(d,p) level. The $(\epsilon^1_{\text{SOMO}} - \epsilon^2_{\text{SOMO}})$ energies are very low except for **6**. The difference $(\epsilon^1_{\text{SOMO}} - \epsilon^2_{\text{SOMO}})$ decreases with increase in length of the linear acenes (**1**−**5**). The degeneracy of the SOMOs for **2**, **10**, and **11** arises accidentally. The molecular point group is C_2 (see Table 5) that is abelian. The rest of the diradicals undergo a distortion from this symmetry.

That all the diradicals have SOMO−SOMO energy difference less than 1.5 eV and all have ferromagnetic ground states is in agreement with the empirical rule proposed by Hoffmann.[31]

Isotropic Hyperfine Coupling Constant (hfcc). The polarized continuum model (PCM) has been successfully applied to the investigation of the isotropic hyperfine coupling constant (a_N) of organic radicals in solution. The solute−solvent interaction can change a_N values by modifying the local spin density. In this work, we have calculated a_N values for all four equivalent N atoms in each diradical.

The hfcc of the two equivalent nitrogen atoms in nitronyl nitroxide monoradicals with different substitutions at α-carbon atoms is in the range of 7.00−7.81 G.[32] The hfcc does not

strongly depend on the nature of the substitution at the α-position, but solvents play a significant role. For diradicals with conjugated couplers, hfcc values decrease to half of the values for the corresponding monoradicals. The experimental values lie in the range of 3−4.5 G for diradicals with different couplers.[33] Cirujeda et al.[34] calculated the hfcc for several α-nitronyl aminoxyl radicals by the B3LYP method using EPR-II basis sets. They found similar hfcc for the monoradicals with similar steric constraints between the two rings. Thus the spin density distribution in the phenyl ring is not strongly dependent on the nature and position of substituents. In our previous work a detailed discussion was given on this issue.[35]

In this work, we have calculated the hfcc for the diradical in the gas phase as well as in three different solvents. The calculated average hfcc values for the N atoms are given in Table 6. A detailed table is given as Supporting Information. The average a_N values for the nitrogen atoms are in good agreement with the experimental values for general nitronyl nitroxide diradicals. The calculated values indicate that there is a preference for the spin density to localize on one of the N atoms in each NN moiety.

Solvent plays an important role in hfcc. In all the species, the hfcc values for N atoms increase with the increase in dielectric constant. For linear acenes (**1**−**5**), the average hfcc value increases as the coupler size increases. However, a straightforward correlation of the a_N values with the calculated J remains missing.

5. Conclusions

The magnetic exchange coupling constants are calculated for eleven diradicals by the broken-symmetry density functional method. The coupling constant J is found to decrease for the linear acene couplers from one to three benzenoid rings, but it increases from three to five benzenoid rings. The α-HOMO and β-HOMO are not the only magnetically active orbitals for **3**−**5**. This happens due to the increase of the diradical character of the acene couplers. The diradical character is lost in the bent couplers. The NICS value at the central rings of the linear acene is high, while the terminal rings lose the benzenoid character. The J value increases with BO, and decreases with the increase in the angle of twist of the NN monoradicals from the coupler plane. The qualitatively proposed eq 7 can give a fair estimate of J. Reliable a_N values are obtained for the diradicals in solution.

Polyacene Spacers in Intramolecular Magnetic Coupling

J. Phys. Chem. A, Vol. 110, No. 49, 2006 **13237**

Supporting Information Available: The optimized coordinates of all the diradicals and complete table for a_N. This material is available free of charge via the Internet at http://pubs.acs.org.

References and Notes

(1) (a) Kahn, O. *Molecular Magnetism*; VCH: New York, 1993. (b) Benelli, C.; Gatteschi, D. *Chem. Rev.* **2002**, *102*, 2369.

(2) (a) Blundell, S. J.; Pratt, F. L. *J. Phys.: Condens. Matter* **2004**, *16*, R771. (b) Luneau, D.; Rey, P. *Coord. Chem. Rev.* **2005**, *249*, 2591.

(3) Blundell, S. J.; Pratt, F. L. *J. Phys.: Condens. Matter* **2004**, *16*, R771.

(4) Tamura, M.; Nakazawa, Y.; Shiomi, D.; Nozawa, K.; Hosokoshi, Y.; Ishikawa, M.; Takahashi, M.; Kinoshita, M. *Chem. Phys. Lett.* **1991**, *186*, 401.

(5) Nakazawa, Y.; Tamura, M.; Shirakawa, N.; Shiomi, D.; Takahashi, M.; Kinoshita, M.; Ishikawa, M. *Phys. Rev. B* **1992**, *46*, 8906.

(6) (a) Wautelet, P.; Le Moigne, J.; Videva, V.; Turek, P. *J. Org. Chem.* **2003**, *68*, 8025. (b) Catala, L.; Le Moigne, J.; Gruber, N.; Novoa, J. J.; Rabu, P.; Belorizky, E.; Turek, P. *Chem. Eur. J* **2005**, *11*, 2440.

(7) Barone, V.; Bencini, A.; Matteo, A. d. *J. Am. Chem. Soc.* **1997**, *119*, 10831.

(8) (a) Ziessel, R.; Stroh, C.; Heise, H.; Köehler, F. K.; Turek, P.; Claiser, N.; Souhassou, M.; Lecomte, C. *J. Am. Chem. Soc.* **2004**, *126*, 12604. (b) Stroh, C.; Ziessel, R.; Raudaschl-Sieber, G.; Köehler, F.; Turek, P. *J. Mater. Chem.* **2005**, *15*, 850.

(9) Vyas, S.; Ali, Md. E.; Hossain, E.; Patwardhan, S.; Datta, S. N. *J. Phys. Chem. A* **2005**, *109*, 4213.

(10) Ali, Md. E.; Datta, S. N. *J. Phys. Chem. A* **2006**, *110*, 2776.

(11) (a) Hegmann, F. A.; Tykwinski, R. R.; Lui, K. P. H.; Bullock, J. E.; Anthony, J. E. *Phys. Rev. Lett.* **2002**, *89*, 227403. (b) Meng, H.; Bendikov, M.; Mitchell, G.; Helgeson, R.; Wudl, F.; Bao, Z.; Siegrist, T.; Kloc, C.; Chen, C.-H. *Adv. Mater.* **2003**, *15*, 1090.

(12) Raghu, C.; Patil, Y. A.; Ramasesha, S. *Phys. Rev. B* **2002**, *65*, 155204.

(13) (a) Lahti, P. M.; Ichimura, A. S. *J. Org. Chem.* **1991**, *56*, 3030. (b) Ling, C.; Minato, M.; Lahti, P. M.; van Willigen, H. *J. Am. Chem. Soc.* **1992**, *114*, 9959. (c) Minato, M.; Lahti, P. M. *J. Am. Chem. Soc.* **1997**, *119*, 2187.

(14) Ovchinnikov, A. A. *Theor. Chim. Acta* **1978**, *47*, 297.

(15) (a) Klein, D. J. *Pure Appl. Chem.* **1983**, *55*, 299. (b) Klein, D. J.; Alexander, S. A. In *Graph Theory and Topology in Chemistry*; King, R. B., Rouvay, D. H., Eds.; Elsevier: Amsterdam, The Netherlands, 1987; Vol. 51, p 404.

(16) Borden, W. T.; Davidson, E. R. *J. Am. Chem. Soc.* **1977**, *99*, 4587.

(17) Shen, M.; Sinanŏglu, O. In *Graph Theory and Topology in Chemistry*; King, R. B., Rouvay, D. H., Eds.; Elsevier: Amsterdam, The Netherlands, 1987; Vol. 51, p 373.

(18) (a) Nachtigall, P.; Jordan, K. D. *J. Am. Chem. Soc.* **1992**, *114*, 4743. (b) Nachtigall, P.; Jordan, K. D. *J. Am. Chem. Soc.* **1993**, *115*, 270.

(19) (a) Noodleman, L. *J. Chem. Phys.* **1981**, *74*, 5737. (b) Noodleman, L.; Baerends, E. J. *J. Am. Chem. Soc.* **1984**, *106*, 2316. (c) Noodleman, L.; Peng, C. Y.; Case, D. A.; Mouesca, J.-M. *Coord. Chem. Rev.* **1995**, *144*, 199.

(20) Ginsberg, A. P. *J. Am. Chem. Soc.* **1980**, *102*, 111.

(21) Noodleman, L.; Davidson, E. R. *Chem. Phys.* **1986**, *109*, 131.

(22) (a) Bencini, A.; Totti, F.; Daul, C. A.; Doclo, K.; Fantucci, P.; Barone, V. *Inorg. Chem.* **1997**, *36*, 5022. (b) Bencini, A.; Gatteschi, D.; Totti, F.; Sanz, D. N.; Mc Clevrty, J. A.; Ward, M. D. *J. Phys. Chem. A* **1998**, *102*, 10545.

(23) Ruiz, E.; Cano. J.; Alvarez, S.; Alemany, P. *J. Comput. Chem.* **1999**, *20*, 1391.

(24) (a) Martin, R. L.; Illas, F. *Phys. Rev. Lett.* **1997**, *79*, 1539. (b) Caballol, R.; Castell, O.; Illas, F.; Moreira, I. d. P. R.; Malrieu, J. P. *J. Phys. Chem. A* **1997**, *101*, 7860. (c) Barone, V.; Matteo, A. d.; Mele, F.; Moreira, I. d. P. R.; Illas, F. *Chem. Phys. Lett.* **1999**, *302*, 240. (d) Illas, F.; Moreira, I. d.P. R.; Graaf, C. d.; Barone, V. *Theor. Chem. Acc.* **2000**, *104*, 265.

(25) (a) Yamaguchi, K.; Takahara, Y.; Fueno, T.; Nasu, K. *Jpn. J. Appl. Phys.* **1987**, *26*, L1362. (b) Yamaguchi, K.; Jensen, F.; Dorigo, A.; Houk, K. N. *Chem. Phys. Lett.* **1988**, *149*, 537. (c) Yamaguchi, K.; Takahara, Y.; Fueno, T.; Houk, K. N. *Theor. Chim. Acta* **1988**, *73*, 337.

(26) Frisch, M. J.; Trucks, G. W.; Schlegel, H. B.; Scuseria, G. E.; Robb, M. A.; Cheeseman, J. R.; Montgomery, J. A., Jr.; Vreven, T.; Kudin, K. N.; Burant, J. C.; Millam, J. M.; Iyengar, S. S.; Tomasi, J.; Barone, V.; Mennucci, B.; Cossi, M.; Scalmani, G.; Rega, N.; Petersson, G. A.; Nakatsuji, H.; Hada, M.; Ehara, M.; Toyota, K.; Fukuda, R.; Hasegawa, J.; Ishida, M.; Nakajima, T.; Honda, Y.; Kitao, O.; Nakai, H.; Klene, M.; Li, X.; Knox, J. E.; Hratchian, H. P.; Cross, J. B.; Adamo, C.; Jaramillo, J.; Gomperts, R.; Stratmann, R. E.; Yazyev, O.; Austin, A. J.; Cammi, R.; Pomelli, C.; Ochterski, J. W.; Ayala, P. Y.; Morokuma, K.; Voth, G. A.; Salvador, P.; Dannenberg, J. J.; Zakrzewski, V. G.; Dapprich, S.; Daniels, A. D.; Strain, M. C.; Farkas, O.; Malick, D. K.; Rabuck, A. D.; Raghavachari, K.; Foresman, J. B.; Ortiz, J. V.; Cui, Q.; Baboul, A. G.; Clifford, S.; Cioslowski, J.; Stefanov, B. B.; Liu, G.; Liashenko, A.; Piskorz, P.; Komaromi, I.; Martin, R. L.; Fox, D. J.; Keith, T.; Al-Laham, M. A.; Peng, C. Y.; Nanayakkara, A.; Challacombe, M.; Gill, P. M. W.; Johnson, B.; Chen, W.; Wong, M. W.; Gonzalez, C.; Pople, J. A. *Gaussian 03*; Gaussian, Inc.: Pittsburgh, PA, 2003.

(27) (a) Bendikov, M.; Duong, H. M.; Starkey, K.; Houk, K. N.; Carter, E. A.; Wudl, F. *J. Am. Chem. Soc.* **2004**, *126*, 7416. (b) Constantinides, C. P.; Koutentis, P. A.; Schatz, J. *J. Am. Chem. Soc.* **2004**, *126*, 16232.

(28) Wiberg, K. *Tetrahedron* **1968**, *24*, 1083.

(29) (a) Schleyer, P. v. R.; Maerker, C.; Dransfeld, A.; Jiao, H.; Hommes, N. J. R. v. E. *J. Am. Chem. Soc.* **1996**, *118*, 6317. (b) Chen, Z.; Wannere, C. S.; Corminboeuf, C.; Puchta, R.; Schleyer, P. v. R. *Chem. Rev.* **2005**, *105*, 3842. (c) Schleyer, P. v. R.; Manoharan, M.; Jiao, H.; Stahl, F. *Org. Lett.* **2001**, *3*, 3643.

(30) Shiomi, D.; Tamura, M.; Sawa, H.; Kato, K.; Kinoshita, H. *Synth. Met.* **1993**, *56*, 3279.

(31) Hoffmann, R.; Zeiss, G. D.; Van Dine, G. W. *J. Am. Chem. Soc.* **1968**, *90*, 1485.

(32) (a) D'Anna, J. A.; Wharton, J. H. *J. Chem. Phys.* **1970**, *53*, 4047. (b) Jurgens, O.; Cirujeda, J.; Mas, M.; Mata, I.; Cabrero, A.; Vidal-Gancedo, J.; Rovira, C.; Molins, E.; Veciana, J. *J. Mater. Chem.* **1997**, *7*, 1723. (c) Zeissel, R.; Ulrich, G.; Lawson, R. C.; Echegoyen, L. *J. Mater. Chem.* **1999**, *9*, 1435. (d) Shiomi, D.; Sato, K.; Takui, T.; Itoh, K.; Tamura, M.; Nishio, Y.; Kajita, K.; Nakagawa, M.; Ishida, T.; Nogami, T. *Mol. Cryst. Liq. Cryst.* **1999**, *335*, 359.

(33) (a) Luckhurst, G. R. In *Spin Labeling. Theory and applications*; Berliner, J. L., Ed.; Academic Press: New York, 1976; p 133 ff. (b) Luckhurst, G. R.; Pedulli, G. F. *J Am. Chem. Soc.* **1970**, *92*, 4738. (c) Dulog, L.; Kim, J. S. *Makromol. Chem.* **1989**, *190*, 2609. (d) Catala, L.; Le Moigne, J.; Kyritsakas, N.; Rey, P.; Novoa, J. J.; Turek, P. *Chem. Eur. J* **2001**, *7*, 2466.

(34) Cirujeda, J.; Vidal-Gancedo, J.; Jürgens, O.; Mota, F.; Novoa, J. J.; Rovira, C.; Veciana, J. *J. Am. Chem. Soc.* **2000**, *122*, 11393.

(35) Ali, Md. E.; Vyas, S.; Datta, S. N. *J. Phys. Chem. A* **2005**, *109*, 6272.